Converting CESR Into A Frontier Hard X-Ray Light Source

R. Talman, D. Rubin, Lab. of Elementary Particle Physics, Cornell University, Ithaca, NY 14850, USA

Abstract

The relatively large horizontal emittance ϵ_x of CESR, an electron storage ring designed for colliding beam operation, does not limit its performance after its conversion into a frontier x-ray source, CESR-X. Its flexible lattice optics permits the production of hard x-ray beams competitive with any in the world by exploiting the fact that the conditions required for Liouville's theorem to be valid are applicable to charged particle focusing but *not* to x-ray focusing. X-ray focusing (with currently available devices) causes an increase in electron beam "effective" emittance that would prevent even a fourth generation source, such as an ERL, from outperforming the existing CESR-X ring as a source of hard x-rays. As x-ray focusing devices are improved this will become less true and it will be important for CESR-X to keep pace. A plan for doing this is described.

DOWNSTREAM VIRTUAL WAIST

We consider only beams produced from undulators (length L_u, parameter K, period λ_u). Such sources are usually placed at electron beam waists in storage rings; here referred to as "waist at undulator" operation. To be emphasized is the superiority of "downstream virtual waist" operation[1] in which the storage ring optics are adjusted so that, as electrons pass through the undulator, they are aimed toward a downstream waist. "Good" radiated photons (those in the 0.1% bandwidth at the edge of the spectrum from undulator harmonic $n_{\rm harm}$ (an odd integer) are also, therefore, aimed toward their intended downstream target. The waist is virtual since the electrons themselves never pass through it. The optimal virtual waist location depends on the x-ray experiment being served. To simplify formulas it will be assumed here that the beam waist is located at position $z = L/2$, half way along a beamline of length L. To achieve this the beta function variation along the beamline is given (in both transverse planes) by

$$\beta = L/2 + (z - L/2)^2/(L/2) \qquad (1)$$

Exactly forward emitted photons (precisely the good ones) inherit the electron's beta functions. Their transverse coordinates x^*, just before the downstream target, are distributed identically to the displacements x_u of electrons at the upstream source. Optionally the x-ray beam is focused to a much narrower distribution in photon displacement x^{**}at the target. A sketch of the beamline is shown in Figure 1. As drawn the focusing device is an ellipsoidal mirror, but some other focusing device could be used instead. Other required elements, such as a monochromator, are not shown.

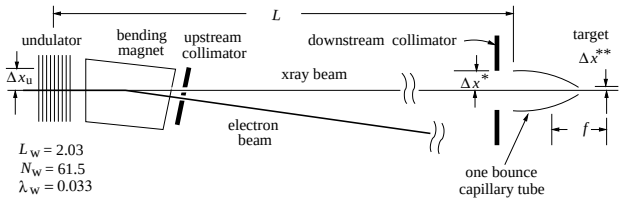

Figure 1: Idealized beamline layout

Beam widths are in the millimeter range at the downstream collimator; focused beam widths are in the ten micrometer range. For some experiments, such as inelastic scattering or those requiring high coherence, the focusing is not needed, but focusing is needed for microbeams. Surprisingly, in the latter case, the beamline design is dictated by the achievable r.m.s. mirror slope error $\sigma'_{\rm mirror}$ (which we take to be 2.0e-5)[2] and by the numerical aperture limit (for x-ray energy E_γ, it is $NA = 1/(20E_{\rm gamma}[{\rm keV}])$ imposed by the need for total external reflection from the mirror. (Slope errors an order of magnitude smaller than this have been achieved with K-B mirrors but, without collimation, aberrations from the unfavorable K-B geometry contribute comparably to spot sizes.) We constrain the beamline design such that the contributions to focused spot size Δx^{**} coming from ϵ_x and from $\sigma'_{\rm mirror}$ are equal. Reducing ϵ_x (even to zero) from this condition has little effect on either the flux density or the spot size. From Eq. (1) and the above constraints, one derives mirror focal length f and pre- and post- mirror spot sizes:

$$\begin{aligned} f &= 40\sigma'_{\rm mirror}E_\gamma[{\rm keV}]L \\ \Delta x^* &= 2\sigma'_{\rm mirror}L \\ \Delta x^{**} &= 80\,\sqrt{2}\,\sigma'^2_{\rm mirror}\,E_\gamma[{\rm keV}]L \end{aligned} \qquad (2)$$

The mirror aperture radius is slightly larger than Δx^* and the downstream collimator is slightly larger again. Most of the good photons emitted from the undulator survive to pass through the focal spot, potentially to register as experimental counts. Upstream collimation can reduce the size of the spot (which is the image of the upstream collimator) at the cost of both flux and flux density. For perfect (respectful of Liouville's theorem) focusing, the focal spot size is given by

$$x^{**} = 20E_\gamma[{\rm keV}]\epsilon_x. \qquad (3)$$

This relation may seem to vindicate treating ϵ_x as the definitively useful figure of merit for the electron beam. But this is misleading since, at least superficially, Eqs. (2) are *independent* of ϵ_x. But this too is misleading, since the ability to meet the constraints on which Eqs. (2) are based

depends on ϵ_x. The condition to be met by the electron beam is

$$\epsilon_x \beta_x < 4\sigma'^2_{\rm mirror} L^2. \quad (4)$$

Using the current operating value for ϵ_x, to (just) satisfy condition (4) requires $L = \beta_x = 31.1\,$m. Both of these conditions are readily achievable without physical changes to the CESR lattice; this defines Phase I, CESR-X operation as shown in Figure 2. The 2mm long undulator replaces an electrostatic separator. Both horizontal and vertical β-functions are near 31 m and the α-functions are adjusted for virtual waist 30 m downstream. Parameters for

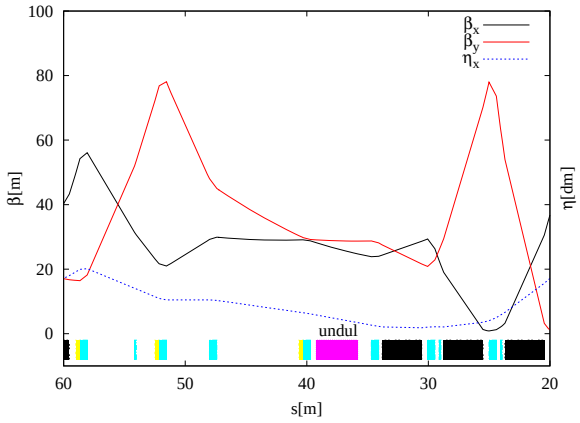

Figure 2: Waist-downstream, Phase I, lattice optics

the leading undulator harmonics are shown in Table 1. Because the spot dimensions are of micrometer scale, square-micrometer units are used for flux densities. Conventional (square-millimeter based) flux densities would be 10^6 times larger. As x-ray focusing devices improve beyond the current state of the art, or to service other, potentially more faithful, probably chromatic, focusing devices, such as Fresnel zone plates or refractive lenses, it will become progressively harder to meet condition (4). But, even without significant alterations, β_x values as great as 100m, along with $L = \beta_x$ are practical. It is straightforward to rearrange the layout of the guide field magnets, in what is now the hard bend region, to be compatible with a 19 m long, zero dispersion drift space suitable for insertion devices. The lattice functions can then be manipulated to match β-functions for 20 m$< L <$ 100 m. An example of CESR-X west area lattice optics with $\beta_x = \beta_y = 100\,$m, zero dispersion and downstream waists is shown in Figure 3. Also the CESR-X emittance can be reduced by a factor of 7 with relatively inexpensive changes to the lattice and vacuum chamber while retaining all other laboratory infrastructure. We reuse a fraction of the arc bends and some 100 additional quads in a TME-style configuration to achieve the emittance reduction.

MONOCHROMATIC COLLIMATION

Inelastic x-ray scattering (IXS), for example, requires extremely small absolute energy bandwidth. Paradoxically,

Table 1: Parameters of beamline with mirror aperture matched to horizontal beam width. "¶" is abbreviation for "ph/s/0.1%BW". "§" is abbreviation for "ph/s/0.1%BW/square-μm". Mirror imperfection is especially significant for bold face entries.

parameter	symbol	unit	value
electron energy	E_e	GeV	5.11
electron current	$I_{\rm av}$	A	0.5
beamline length	L	m	31.1
$n_{\rm harm} = 1$, E_γ		keV	3.36
flux	Φ_1	¶	1.09e15
flux density**	Φ_1/A_1^{**}	§	2.18e13
$n_{\rm harm} = 3$, E_γ		keV	10.09
focal length	f	m	0.251
magnification	M		0.00809
pre-focus beam half width	$\Delta x^*/y^*$	μm	1247/55.8
spot half width (ideal)	$\Delta x^{**}/y^{**}$	μm	**10.1/0.45**
spot half width (broadened)	$\widetilde{\Delta x}^{**}/y^{**}$	μm	**14.2/10.1**
flux	Φ_3	¶	3.92e14
flux density**	Φ_3/A_3^{**}	§	8.69e11
$n_{\rm harm} = 5$, E_γ		keV	16.81
flux	Φ_5	¶	1.62e14
flux density**	Φ_5/A_5^{**}	§	1.29e11
$n_{\rm harm} = 7$, E_γ		keV	23.53
flux	Φ_7	¶	8.10e13
flux density**	Φ_7/A_7^{**}	§	3.30e10
$n_{\rm harm} = 9$, E_γ		keV	30.25
flux	Φ_9	¶	2.79e13
flux density**	Φ_9/A_9^{**}	§	6.88e9

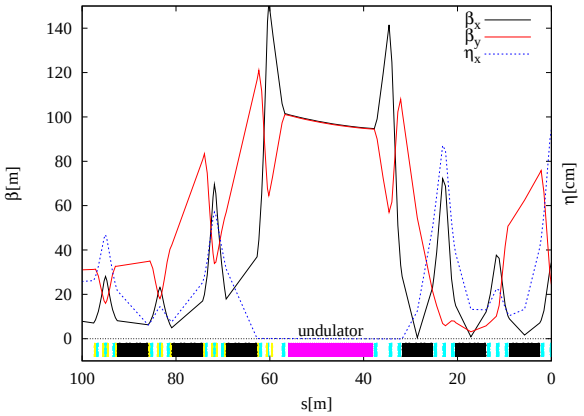

Figure 3: Waist-downstream, Phase II, lattice optics.

multi-crystal monochromators capable of producing milli-eV energy spread favor high x-ray energies of order 20 keV. To minimize heat load on such devices it is appropriate to design an optics free beamline that reduces the beam energy spread. Because of the correlation between radiation angle and x-ray energy, collimation automatically provides some degree of monochromatization. This section investigates the performance of CESR-X in this role.

Downstream waist operation is especially favorable for minimizing the energy spread of the beam passing through a downstream collimator. An ultralow emittance source, such as an ERL, is essentially a point source both horizontally and vertically, for which upstream collimation is both

not useful and not necessary. Vertically, CESR-X is similar in this regard, but the CESR-X beam is undesirably wide for most purposes. To reduce heat load on downstream optics it is therefore sensible to reduce the beam width by upstream collimation, with proportional loss of flux. There is, however, little benefit in making the collimated width smaller upstream than downstream. We therefore assume symmetric horizontal upstream and downstream collimation. A ten-fold loss of flux due to this collimation can, for example, be regarded as a roughly ten-fold decrease in electron beam emittance. The photon beam beta function has to be reduced in the same ratio to reflect the altered beam phase space aspect ratio.

With all electrons well aimed toward the target, their radiated photons passing through a tiny downstream collimator are quite monochromatic. In the following figures, waist at undulator, ϵ_x=0.1 nm, I=0.05 A ERL operation is compared to ϵ_x=7 nm CESR-X operation for E_e=5.11 GeV, I=0.5A, L=55m, E_γ=21.7[keV], λ_u=0.018 m, L_u=5 m. Emphasis is on IXS application. Flux is quoted in photons per meV; the conventional (per 0.1% BW) fluxes are 2x10^4 times larger. The beamline has no x-ray focusing and no harmonic filtering, (but the figures include only $N_{\rm harm.}$=3 flux).

Fig. 4 compares β-function variations (the same for horizontal and vertical) along the beam line. CESR-X flexibility enables its more favorable β function variation. The.vertical β function may need to be as much as a factor of two smaller for operational reasons, causing an acceptably small performance penalty. Figures 5 compare CESR-

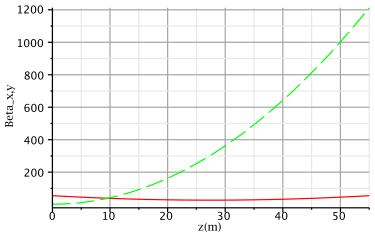

Figure 4: β variation along beamline, both horizontal and vertical. CESR-X solid, ERL broken line. The inferior waist-at-undulator performance is due to the very large β-function (also known as Rayleigh range function) at the downstream target location.

X and ERL on the basis of measures of flux. Part (a) compares dependence of flux (ph/s/meV) on collimator area. Part (b) compares delendence of flux density (ph/s/meV/sq-mm) on collimator area. The maximum collimator area in these plots corresponds, roughly, to a square aperture with 250 μm sides. The stronger than linear dependence on collimator area for CESR-X is due to the proportional increase of upstream collimation area as the downstream aperture area is increased. However, the monochromatization by collimation erodes proportional to the collimation area.

The energy spread of the transmitted beam can be crudely estimated as follows. The parameter $\eta = (E_\gamma(0) - E_\gamma(\theta))/E_\gamma(\vartheta)$ gives the fractional energy offset (from central value) an x-ray has by virtue of its radiation angle ϑ away from the electron direction. η is given approximately by

$$\eta = \tilde{\gamma}_e^2 \vartheta^2, \quad \text{where} \quad \tilde{\gamma}_e^2 = \frac{\gamma_e^2}{1 + K^2/2}. \qquad (5)$$

Including the x-ray energy bandwidth broadening due to electron beam energy spread, the beam transmitted through this collimator has energy bandwidth approximating the "nominal" 0.1%BW, entering the conventional definitions of x-ray brightness and brilliance. Figures 6(a) and (b) compare, respectively, the beam power through collimator and the flux divided by beam power, as functions of collimator area. The latter measure is especially important when radiation heating of beamline equipment limits the data collection rate. By this measure CESR-X and ERL performances are roughly equivalent.

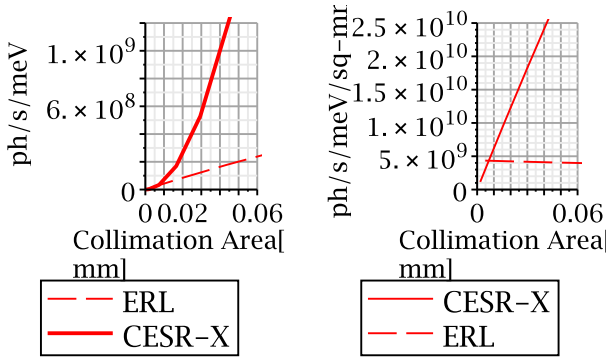

Figure 5: (a) Flux vs area. (b) Flux density vs area.

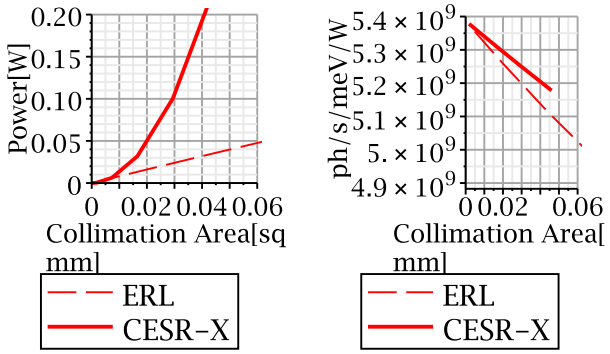

Figure 6: (a) Beam power versus area. (b) Flux per watt.

REFERENCES

[1] C. Liu et al., "Optimal Focusing for Linac-Based Hard X-Ray Source", paper submitted to this PAC meeting

[2] X. Zeng et al. "Ellipsoidal and Parabolic Glass Capillaries as Condensers for X-Ray Microscopes", Applied Optics, Vol. 47, No. 13, 2008